Noncausal Modeling and Closed-Loop Optimal Input Design

Cross-Directional Processes of a Paper Machine

Qiugang Lu, **Lee Rippon**, Bhushan Gopaluni, Michael Forbes, Philip Loewen, Johan Backstrom and Guy Dumont

The University of British Columbia
Pulp and Paper Center

May 25, 2017

Outline

Introduction

The paper machine

- Transforms a slurry of pulp fiber into a uniform sheet of paper through a series of dewatering and pressing operations.
- Can be over 100 m long in the machine-direction (MD), producing a sheet over 10 m wide in the cross-direction (CD) at rates exceeding 30 m/s [1].

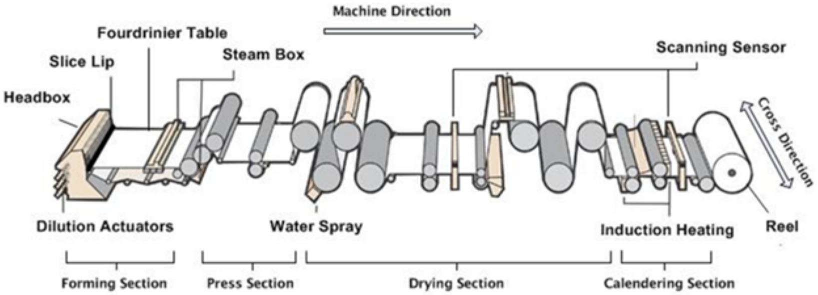

Figure 1: Schematic of a Fourdrinier paper machine [3]

Introduction

CD actuators

- Spatial variations are controlled by CD actuators distributed across the width of the paper machine.
- Headbox dilution profiling valves and induction heating profilers are two primary CD actuators.

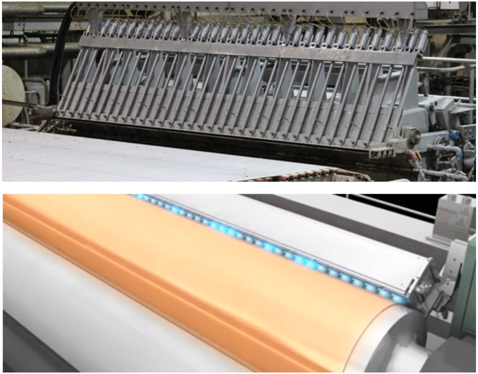

Figure 2: Headbox dilution valves (top) and induction profilers (bottom)

Cross-Directional Process

Steady-state model

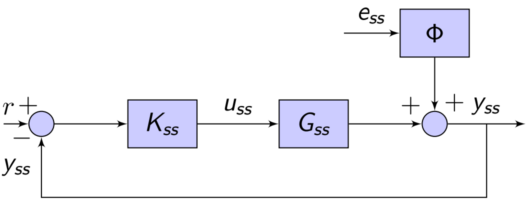

Figure 3: Closed-loop control system

$$y_{ss} = G_{ss} u_{ss} + \Phi e_{ss}, \tag{1}$$

where each column of $G_{ss} \in \mathbb{R}^{m \times m}$ is the sampled impulse response (IR) of a single actuator and all actuators are assumed to have identical and symmetric IR coefficients.

$$K_{ss} = -Q_3^{-1} \alpha_K G_{ss} Q_1, \tag{2}$$

where Q_1 and Q_3 are weighting matrices that penalize deviation from set-point and steady-state MV offset, respectively.

Cross-Directional Process

Closed-loop

- MPC (K_{SS}) assumed to operate linearly with no active constraints.
- We have the following closed-loop CD process:

$$\begin{aligned} y_{ss} &= (I + G_{ss}K_{ss})^{-1} G_{ss}K_{ss}r + (I + G_{ss}K_{ss})^{-1} v_{ss}, \quad (3) \\ u_{ss} &= (I + K_{ss}G_{ss})^{-1} r - (I + K_{ss}G_{ss})^{-1} K_{ss}v_{ss}, \quad (4) \end{aligned}$$

  where $r \in \mathbb{R}^m$ is the spatial excitation signal to be designed.
- **Challenge:** Large input-output dimensions and large number of parameters in G_{ss}.
- **Solution:** Use a noncausal scalar transfer function to represent steady-state CD actuator response and reduce complexity.

Causal Scalar Representation

Noncausal Scalar Model

- Scalar noncausal finite IR (FIR) model from any column of G_{ss} represents spatial impulse response of an actuator, i.e.,

$$g(\lambda, \lambda^{-1}) = g_{-n}\lambda^{-n} + \ldots + g_0 + \ldots + g_n\lambda^n, \tag{5}$$

where $n < m$ is a truncated index representing significant coefficients and $g_i = g_{-i}$.

- n is large so a parsimonious noncausal transfer function is used to approximate $g(\lambda, \lambda^{-1})$ as

$$\begin{aligned}
\bar{g}(\lambda, \lambda^{-1}) &= \frac{B(\lambda)B(\lambda^{-1})}{A(\lambda)A(\lambda^{-1})}, & (6)\\
B(\lambda^{-1}) &= b_0 + b_1\lambda^{-1} + \ldots + b_{n_b}\lambda^{-n_b}, & (7)\\
A(\lambda^{-1}) &= 1 + a_1\lambda^{-1} + \ldots + a_{n_a}\lambda^{-n_a}, & (8)
\end{aligned}$$

where n_a and n_b are the orders of $A(\lambda^{-1})$ and $B(\lambda^{-1})$, respectively.

Causal Scalar Representation

Noncausal Scalar Model

- Similarly for $k(\lambda, \lambda^{-1})$ we have

$$\bar{k}(\lambda, \lambda^{-1}) = \frac{F(\lambda)F(\lambda^{-1})}{E(\lambda)E(\lambda^{-1})}, \tag{9}$$

$$F(\lambda^{-1}) = f_0 + f_1\lambda^{-1} + \ldots + f_{n_f}\lambda^{-n_f}, \tag{10}$$

$$E(\lambda^{-1}) = 1 + e_1\lambda^{-1} + \ldots + e_{n_e}\lambda^{-n_e}, \tag{11}$$

  where n_e and n_f are the orders of $E(\lambda^{-1})$ and $F(\lambda^{-1})$, respectively.

- High dimensional MIMO steady-state closed-loop model replaced by scalar noncausal transfer functions, i.e.,

$$y(x) = \frac{\bar{g}}{1 + \bar{g}\bar{k}} r(x) + \frac{1}{1 + \bar{g}\bar{k}} v(x), \tag{12}$$

$$u(x) = \frac{1}{1 + \bar{g}\bar{k}} r(x) - \frac{\bar{k}}{1 + \bar{g}\bar{k}} v(x), \tag{13}$$

  where x stands for the spatial coordinate.

Causal Scalar Representation

Causal Equivalent Model

- Consider the following noncausal Box-Jenkins model:

$$y(x) = \frac{M(\lambda)M(\lambda^{-1})}{N(\lambda)N(\lambda^{-1})} r(x) + \frac{R(\lambda)R(\lambda^{-1})}{S(\lambda)S(\lambda^{-1})} e(x), \tag{14}$$

where $\{e(x), x = 1, \ldots, m\}$ is a Gaussian white noise sequence.

- Assuming all polynomials have no zeros on the unit circle and are minimum phase, there exist causal polynomials $\tilde{M}_y(\lambda^{-1})$, $\tilde{N}_y(\lambda^{-1})$, $\tilde{R}_y(\lambda^{-1})$, $\tilde{S}_y(\lambda^{-1})$, a white noise sequence $\{\tilde{e}_y(x)\}$ and a stochastic sequence $\{\tilde{y}(x)\}$ with the same spectra as $\{y(x)\}$ such that,

$$\tilde{y}(x) = \frac{\tilde{M}_y(\lambda^{-1})}{\tilde{N}_y(\lambda^{-1})} r(x) + \frac{\tilde{R}_y(\lambda^{-1})}{\tilde{S}_y(\lambda^{-1})} \tilde{e}_y(x), \tag{15}$$

where $N(\lambda)N(\lambda^{-1})\pi_N = N^2(\lambda^{-1})$, $\tilde{N}(\lambda^{-1}) = N^2(\lambda^{-1})$ and the same also holds for $M(\lambda)$, $R(\lambda)$, and $S(\lambda)$.

Causal Scalar Representation

Causal Equivalent Model

- We have $\tilde{y}(x) = \frac{\pi_M}{\pi_N} y(x)$, $\tilde{e}_y(x) = \frac{\pi_M \pi_S}{\pi_N \pi_R} e(x)$ where $\pi_N = \prod_i \frac{\lambda^{-1} - \beta_i}{\lambda - \beta_i}$ and π_M, π_R and π_S are defined in a similar fashion.
- The input signal $u(x)$ can also be represented through causal filters, i.e.,
$$\tilde{u}(x) = \frac{\tilde{M}_u(\lambda^{-1})}{\tilde{N}_u(\lambda^{-1})} r(x) + \frac{\tilde{R}_u(\lambda^{-1})}{\tilde{S}_u(\lambda^{-1})} \tilde{e}_u(x), \tag{16}$$
where $\{\tilde{u}(x)\}$ and $\{u(x)\}$ have the same spectra.

Causal Scalar Representation

Covariance Equivalence

- Consider the noncausal model (θ is the parameter in compact set Ω)

$$y(x) = \bar{g}(\lambda, \lambda^{-1}, \theta)u(x) + \bar{h}(\lambda, \lambda^{-1}, \theta)e(x), \tag{17}$$

  where $e(x)$ is Gaussian white noise and data is generated in closed-loop and all relevant transfer functions are uniformly stable.

- Then, as $m \to \infty$ (m is the number of measurement bins),

$$\sup_{\theta \in \Omega} |\mathcal{L}_y^m(y) - \mathcal{L}_{\tilde{y}}^m(\tilde{y})| \xrightarrow{\text{w.p.1}} 0, \tag{18}$$

$$\sup_{\theta \in \Omega} \left\| \frac{d\mathcal{L}_y^m(y)}{d\theta} - \frac{d\mathcal{L}_{\tilde{y}}^m(\tilde{y})}{d\theta} \right\| \xrightarrow{\text{w.p.1}} 0, \tag{19}$$

  where $\mathcal{L}_y^m(y)$ is the noncausal log-likelihood function and $\mathcal{L}_{\tilde{y}}^m(\tilde{y})$ is the causal-equivalent log-likelihood function [4].

- Therefore, the parameter covariances coincide and we may perform optimal input design based on the causal-equivalent model.

Optimal Input Design

- Split θ as $\theta = [\rho^T \ \eta^T]^T$ and focus on process model parameters (ρ).
- **Objective:** minimize a function of the parameter covariance of ρ, P_ρ, subject to input and output power constraints, i.e.,

$$\min_{\Phi_r(\omega)} \quad f_0(P_\rho(\Phi_r(\omega))) \tag{20}$$

$$s.t. \quad \frac{1}{2\pi}\int_{-\pi}^{\pi} \Phi_u(\omega) d\omega \leq c_u, \tag{21}$$

$$\frac{1}{2\pi}\int_{-\pi}^{\pi} \Phi_y(\omega) d\omega \leq c_y, \tag{22}$$

where c_u and c_y are the power limits on input and output signals.

- Finite dimensional parameterization of Φ_r, i.e.,

$$\Phi_r(\omega) = \sum_{k=-m_c}^{m_c} c_k e^{-j\omega k} \geq 0, \quad \forall\omega, \tag{23}$$

where $c_k, \ k = -m_c, \ldots, m_c$, are the parameters, and m_c is the selected number of parameters [5].

- Choosing $f_0(\cdot)$ to be convex the resulting optimization is convex.

Case Study

- Spatial actuator response is nonlinear with four parameters, i.e., gain (γ), width (ξ), divergence (β), attenuation (α) [2].
- Comparing three methods
  1. **Optimal input design:** causal-equivalent model, excitation amplitude constrained to $\leq \pm 10$.
  2. **Bump excitation:** amplitudes alternate between $+10$ and -10.
  3. **White noise:** designed with the same variance as the optimal input.
- For computational efficiency model orders are specified as $n_b = n_f = 1$ and $n_a = n_e = 2$.
- Process model is identified in 100 Monte-Carlo simulations.

Case Study

- High order models can improve accuracy with a computation cost.

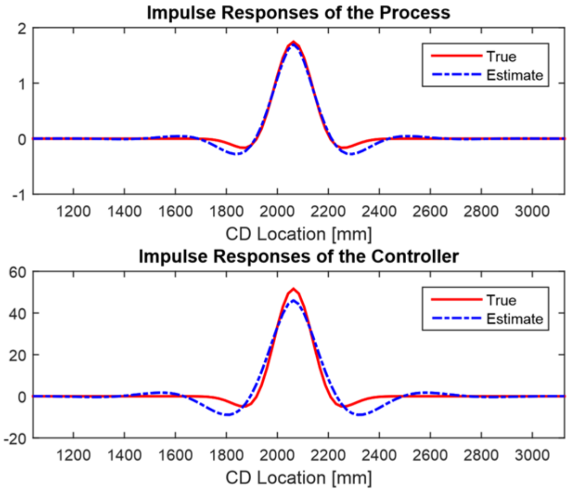

Figure 4: IR of a single actuator (red) and noncausal estimate (blue).

Case Study

- Large spectrum amplitude in the cross-over frequency enables better excitation.

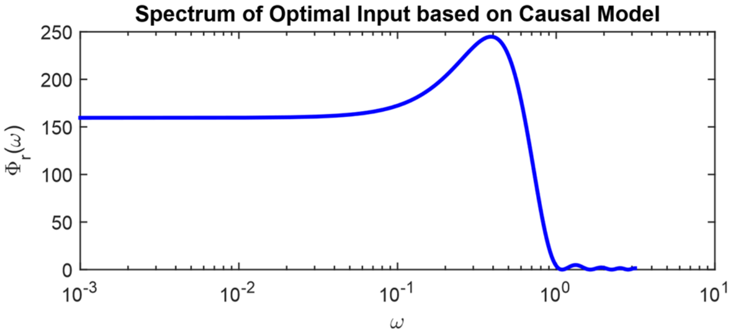

Figure 5: Optimal input spectrum from causal-equivalent model

Case Study

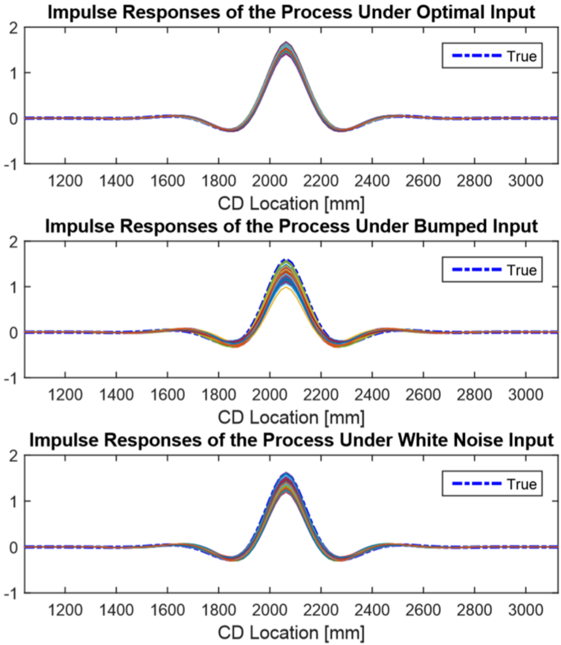
Impulse Responses of the Process Under Optimal Input
True
CD Location [mm]
Impulse Responses of the Process Under Bumped Input
True
CD Location [mm]
Impulse Responses of the Process Under White Noise Input
True
CD Location [mm]

Summary

- Averaged errors ($\bar{\epsilon}$)
  1. **Optimal input design:** $\bar{\epsilon} = 0.0643$
  2. **Bump excitation:** $\bar{\epsilon} = 1.3344$
  3. **White noise:** $\bar{\epsilon} = 0.4479$
- **Noncausal model:** circumvents large dimension of MIMO CD process.
- **Causal-equivalent modeling:** facilitates traditional optimal input design methods.

References I

[1] S Aslani, MS Davies, GA Dumont, and GE Stewart.
Estimation of cross and machine direction variations using recursive wavelet filtering.
Pulp and Paper Canada, pages 45–48, 2009.

[2] Danlei Chu, J Backström, C Gheorghe, A Lahouaoula, and C Chung.
Intelligent closed loop cd alignment.
Proc Control System, pages 161–166, 2010.

[3] Danlei Chu, Cristian Gheorghe, Johan Backstrom, Michael Forbes, and Stephen Chu.
Model predictive control and optimization for papermaking processes.
INTECH Open Access Publisher, 2011.

[4] R Bhushan Gopaluni, Philip D Loewen, Mohammed Ammar, Guy A Dumont, and Michael S Davies.
Identification of symmetric noncausal processes: Cross-directional response modelling of paper machines.
In *Decision and Control, 2006 45th IEEE Conference on*, pages 6744–6749. IEEE, 2006.

[5] Henrik Jansson and Håkan Hjalmarsson.
Input design via lmis admitting frequency-wise model specifications in confidence regions.
IEEE transactions on Automatic Control, 50(10):1534–1549, 2005.